Open Charm and Beauty Production at HERA.

Karin Daum [a*]

[a]Rechenzentrum, Universität Wuppertal,
Gaußstraße 20, D-42097 Wuppertal, Germany

Measurements on open charm and beauty production in ep collisions at a centre-of-mass energy of $\sqrt{s} = 300$ GeV performed by the H1 experiment at HERA are presented. Final states containing charm are identified by the reconstruction of $D^{*\pm}$ meson while events containing muons and at least two jets were used to select a data sample enriched with beauty. The results cover the region of four-momentum transfer squared Q^2 from photoproduction ($Q^2 \approx 0$) to deep inelastic scattering at large Q^2. The experimental results are compared with theoretical prediction based on QCD calculations.

1. INTRODUCTION

The study of heavy flavor production in lepton-proton scattering provides an important tool for testing the standard model of strong interactions. At the ep collider HERA, which was operated at a centre-of-mass energy of $\sqrt{s} = 300$ GeV, heavy quarks are almost exclusively produced by the *photon gluon fusion (PGF)* process, $\gamma g \rightarrow Q\overline{Q}$ $(Q = c, b)$, where a real or virtual photon emitted by the electron[2] interacts with a gluon in the proton producing a heavy quark pair $Q\overline{Q}$.

The dominant contribution to heavy flavor production is due to the exchange of an almost real photon *(photoproduction)*, where the negative square of the four-momentum transfer carried by the photon is ($Q^2 \approx 0$). The heavy quarks hadronize and are then either detected as *"open charm (beauty)"*,i.e. with charmed/beauty hadrons, or alternatively as *"hidden charmed (beauty)"* states such as $J/\Psi(\Upsilon)$ visible in the final state.

The kinematics of the ep interaction is described by three independent variables, the centre-of-mass energy $\sqrt{s}$, the four-momentum transfer squared of the photon $q^2 = -Q^2$ and either one of the scaling variables $y = (q \cdot P)/(l \cdot P)$, the inelasticity of the ep interaction, or Bjorken-x $x = Q^2/(2P \cdot l)$. Here P and l denote the four-momentum of the proton and the electron,respectively. The γp centre-of-mass energy squared is given by $W^2_{\gamma p} = W^2 \approx y \cdot s - Q^2$.

Open heavy flavor production at HERA is dominated by charm production. Due to the higher mass and the charge of beauty quarks the cross section for $\sigma(ep \rightarrow eb\overline{b}X)$ is expected to be suppressed by about two orders of magnitude compared to $\sigma(ep \rightarrow ec\overline{c}X)$.Despite of the smallness of the beauty cross section the study of beauty production in lepton nucleon scattering is of special interest because the theoretical calculations of perturbative QCD are expected to be more reliable due to the large scale, i.e. the mass of beauty quarks, involved in beauty production.

The results presented here [1,2] are based on roughly 10 pb^{-1} of data recorded by the H1 [3] in 1995 and 1996 at HERA, when positrons with an energy of 27.5 GeV were collided head-on protons of 820 GeV.

2. OPEN CHARM PRODUCTION

The description of open heavy flavor production is based on perturbative QCD (pQCD). In leading order (LO) the *direct* process of photon gluon fusion, i.e. $\gamma g \rightarrow Q\overline{Q}$ is the dominant contribution. In photoproduction (γp) sizable contributions from *resolved* photon interactions, i.e. $gg \rightarrow Q\overline{Q}$, are expected due to the partonic structure of the photon. In next-to-leading order

*permanent at DESY, Notkestr.85, D-22607 Hamburg, Germany, email: daum@mail.desy.de

[2]Hereafter, a reference to electrons implies a reference to either electrons or positrons.

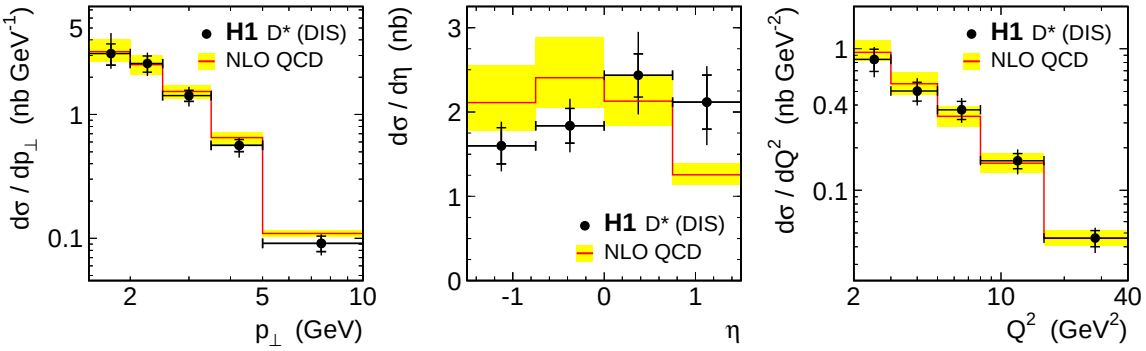

Figure 1. Differential inclusive $D^{*\pm}$ cross sections in DIS (full dots) and NLO QCD prediction (shaded area indicating $1.3 < m_c < 1.7$ GeV).

(NLO) or beyond, however, the resolved photon processes are part of the higher order contributions and the distinction between direct and resolved processes becomes impossible.

Several schemes are used to perform NLO calculations. All approaches assume the scale to be hard enough to apply pQCD and to guarantee the validity of the factorization theorem.

The *massive approach* is a fixed order (in α_s) calculation (FOPT) with massive quarks, i.e. $m_Q \neq 0$, assuming three active flavors in the proton. The heavy quark is only produced at the perturbative level. These calculations are considered reliable in the low $p_\perp$-regime. However, they break down for $p_\perp \gg m_Q$ due to large logarithms $\ln(p_\perp^2/m_Q^2)$. The fragmentation of the heavy quarks into heavy flavored hadrons is taken to be independent from these calculations.

In the *massless approach*[4,5] the charm quark mass is assumed zero and therefore charm is treated as an additional active flavor in the proton. This ansatz of *flavor excitation (FE)* gives rise to new processes like $cg \to cg$, $cq \to cq, \ldots$. Within this approach the final state collinear divergences are absorbed into the fragmentation functions. The massless approach is indispensable for $p_\perp \gg m_Q$, however it breaks down for $p_\perp \leq m_Q$. Both, massive and massless approach have been successfully applied to open charm in photoproduction. In DIS only the FOPT has been used so far [6,7].

In a third approach the features of both methods are combined. The *variable flavor number scheme*(VFNS) adjusts the number of partons N_f in the proton according to the relevant scale. It applies the FOPT with massive quarks at low scales and treats the heavy similar to massless quarks for scales much above m_Q. It has been mainly applied for inclusive quantities such as σ_{tot}, F_2^Q [8] but recently also differential cross sections of charmed hadrons were calculated [9].

2.1. $D^{*\pm}$ Production in DIS

$D^{*\pm}$ mesons are identified by the decay chain $D^{*\pm} \to D^0\pi^\pm$, $D^0 \to K^\mp\pi^\pm$ in the visible range of the transverse momentum $p_\perp(D^*) > 1.5$ GeV and the pseudorapidity $|\eta(D^*)| < 1.5$ in the laboratory frame. For the DIS selection the event kinematics is restricted to $0.05 < y < 0.7$ and $2\ \text{GeV}^2 < Q^2 < 100\ \text{GeV}^2$.

In figure 1 differential inclusive $D^{*\pm}$ cross sections are shown as a function of $p_\perp(D^*)$, $\eta(D^*)$ and Q^2. A comparison to predictions based on massive pQCD in NLO reveals reasonable agreement with the data for $m_c \approx 1.5$ GeV.

2.2. $D^{*\pm}$ in Photoproduction

The inclusive $D^{*\pm}$ analysis in the regime of photoproduction is restricted to events in which the outgoing electron is detected upstream in one of the electron taggers at a distance of 33 and 44 metres from the interaction point. The corresponding kinematic regions for the two data sets are summarized in table 1.

In figure 2 differential inclusive $D^{*\pm}$ photoproduction cross sections are shown as a function of

Table 1
Kinematic regions in photoproduction

	33 m	44 m
Q^2 $[GeV^2]$	< 0.01	< 0.01
$\langle W \rangle$ $[GeV]$	194	88
y	0.29 - 0.62	0.02 - 0.32
$p_\perp(D^*)$ $[GeV]$	2.5	2.0
$\lvert\hat{y}(D^*)\rvert$	1.5	1.5

the transverse momentum $p_\perp(D^*)$ and and the rapidity $\hat{y}(D^*)$ in the laboratory frame at a mean hadronic centre of mass energy $\langle W \rangle$ of 88 GeV and 194 GeV. Figure 2 also includes the theoretical predictions based on massive NLO calculations [10] which agree well with the data.

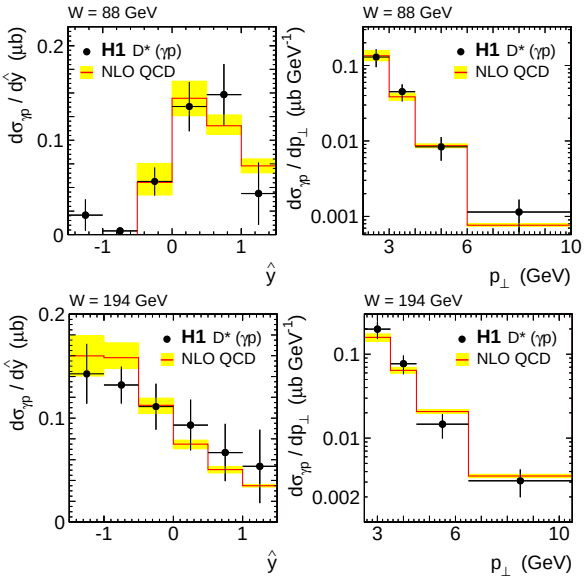

Figure 2. Differential inclusive $D^{*\pm}$ cross sections in photoproduction (full dots) and NLO QCD prediction (shaded area indicating $1.3 < m_c < 1.7$ GeV).

In figure 3 the double differential inclusive $D^{*\pm}$ cross section $\mathrm{d}^2\sigma/\mathrm{d}p_\perp\mathrm{d}\hat{y}$ at $\langle W \rangle = 194$ GeV is compared with predictions based on NLO calculations using the massive and the massless approach, respectively. At small $p_\perp$ significant differences are observed in the predicted cross sections for the different schemes while at larger $p_\perp$ both calculations yield very similar results. As expected the massless approach [5] fails to describe the data at small $p_\perp$. The massive approach is found to agree reasonably well with the data up to $p_\perp \approx 5$ GeV. At larger transverse momenta, however, both calculations predict cross sections in the central rapidity region considerably larger than observed in the data.

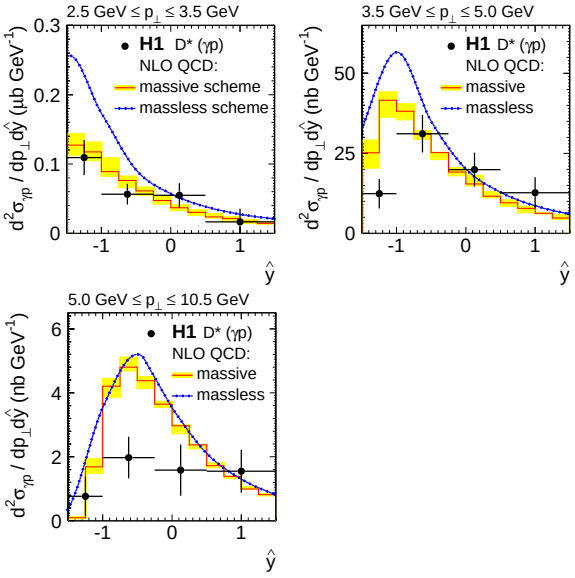

Figure 3. Inclusive $D^{*\pm}$ cross sections $\mathrm{d}^2\sigma/\mathrm{d}p_\perp\mathrm{d}\hat{y}$ in photoproduction (full dots) compared to NLO pQCD prediction in the massless (thick full line) and massive approach (shaded area indicating $1.3 < m_c < 1.7$ GeV).

2.3. Extraction of the Gluon Density

The massive NLO pQCD calculations, which is dominate by PGF, agree in general reasonably well with the measured inclusive $D^{*\pm}$ cross sections, both in γp and in DIS. Moreover, in case of deep inelastic scattering it has been demonstrated explicitly that the data do not allow for a sizeable contribution of charm FE [11]. Although in photoproduction sizeable resolved contributions to heavy flavor production are expected in general, it is possible to suppress them almost completely by restricting the analysis to $\hat{y}(D^*) < 1$.

Therefore the observation of $D^{*\pm}$ mesons allow to tag unambiguously the gluon in the proton in both kinematic regimes.

In the infinite momentum frame the momentum fraction x_g of the proton carried by the gluon is given by

$$x_g = \frac{\hat{s} + Q^2}{ys}. \quad (1)$$

Here $\hat{s}$ denotes the invariant mass of the photon and the gluon or, equivalently, of the outgoing $Q\overline{Q}$ pair. In the photon gluon rest frame $\hat{s}$ may be related to the properties of either of the quarks Q by

$$\hat{s} = \frac{m_Q^2 + p_{\perp Q}^2}{z(1-z)}. \quad (2)$$

Since the photon gluon rest frame is not attainable experimentally $p_{\perp Q}$ has to be approximated by the transverse momentum $p^*_{\perp Q}$ in the hadronic centre of mass system. The inelasticity z may be calculated in the laboratory frame according to

$$z \equiv \frac{P \cdot p_Q}{P \cdot q} = \frac{(E - p_z)_Q^{lab}}{2yE_e}. \quad (3)$$

In the presence of gluon radiation relation (2) and in case of intrinsic $k_\perp$ of the gluon in the proton equations (1,2) are only valid in approximation.

Experimentally the heavy quark Q is not observed directly, but the heavy flavored hadron is measured instead. Therefore in the present analysis the properties of the charm quark are approximated by those of the $D^{*\pm}$ meson and consequently the quantity x_g^{obs} is measured which has to be understood as a convolution of x_g with the approximations mentioned before and the fragmentation of charm quarks into $D^{*\pm}$ mesons.

Figure 4 compares the visible inclusive $D^{*\pm}$ cross section $\mathrm{d}\sigma/\mathrm{d}x_g^{obs}$ with the massive NLO predictions for DIS and for different values of W for photoproduction. A good description of the data is observed.

To obtain the cross section $\mathrm{d}\sigma/\mathrm{d}x_g$ the data are unfolded using the massive NLO programs which allow to determine the correlation between x_g and x_g^{obs} including fragmentation effects. This cross section factorizes as

$$\sigma(x_{g,i}) \sim g(x_{g,i}, \mu_i^2) \cdot \hat{\sigma}(x_{g,i}, \mu_i^2), \quad (4)$$

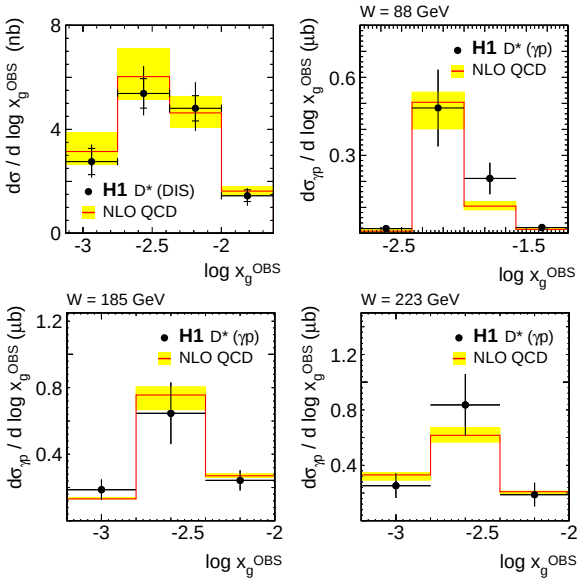

Figure 4. Differential inclusive $D^{*\pm}$ cross section $\mathrm{d}^2\sigma/\mathrm{d}x_g^{obs}$ in DIS and for various values of W in γp (full dots) in comparison to NLO pQCD predictions (shaded area: $1.3 < m_c < 1.7$ GeV).

where $\hat{\sigma}$ and μ denote the partonic NLO cross section and factorization scale, respectively. For each bin i in x_g (and W) the gluon density is probed at a different scale μ_i which depends on the phase space region. At an average scale $\langle\mu\rangle$ the gluon density is obtained by

$$g(x_g, \langle\mu^2\rangle) = g(x_g, \langle\mu^2\rangle)^{theo} \cdot \frac{\sigma(x_{g,i})^{exp}}{\sigma(x_{g,i})^{theo}}, \quad (5)$$

where it is assumed that the gluon density scales with energy as given by the parton density functions (CTEQ4 in DIS and MRST in γp) used for the theoretical calculations. The uncertainty on $g(x_g, \langle\mu^2\rangle)$ introduced by this assumption is included in the systematic errors.

The resulting gluon density distributions are shown in figure 5 for an average scale $\langle\mu^2\rangle = 25\ \mathrm{GeV}^2$ separately for DIS and photoproduction. Good agreement is observed in the gluon density extracted from the cross sections measured in the two different kinematic regimes. These measurements compare also well with the gluon density infered from the QCD analysis of the scaling vi-

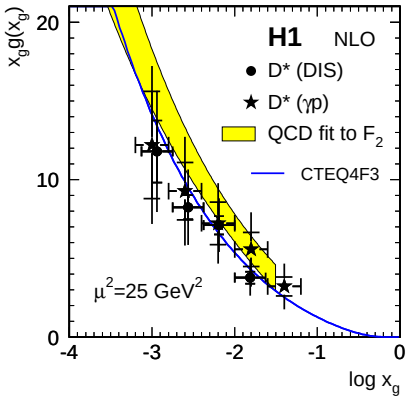

Figure 5. Differential inclusive $D^{*\pm}$ cross section $\mathrm{d}^2\sigma/\mathrm{d}x_g^{obs}$ in DIS and for various values of W in γp (full dots) in comparison to NLO pQCD predictions (shaded area: $1.3 < m_c < 1.7$ GeV).

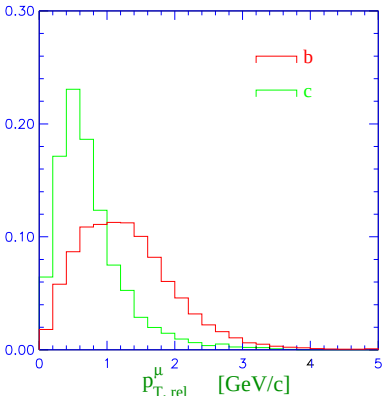

Figure 6. $p_\perp^{\mu\ rel}$ Distributions for charm and beauty events.

olations of F_2. The agreement observed among the the different methods nicely demonstrates the universality of the gluon density in the proton within the framework of NLO pQCD.

3. OPEN BEAUTY PRODUCTION

The analysis of beauty production is based on the semileptonic decay of beauty hadrons resulting in muons identified in the final state. The muon has to be observed in the central region of the detector, i.e. $35^o < \theta^\mu < 130^o$, and its transverse momentum $p_\perp^\mu$ has to exceed 2 GeV. In addition the events have to fulfil the requirement that at least two jets with $E_\perp^{jet} > 6$ GeV are found in the range $|\eta_{jet}| < 2.5$ defining the jets with a cone algorithm with a radius cut of $R = \sqrt{\Delta\eta^2 + \Delta\Phi^2} = 1$. The muon has to be associated with either of the jets. To define the γp-regime it is required that no electron candidate was found with $\theta_e < 177.8^o$, which limits the data sample to $Q^2 < 1$ GeV^2.

Already by these requirements the contribution of beauty events in the selected data sample is significantly enhanced. According to LO Monte Carlo simulations the initial ratio $\sigma(ep \to ec\overline{c}X)$: $\sigma(ep \to eb\overline{b}X)$ of about 200:1 for the full phase space of photoproduction changes to about 2:1.

Finally the statistical separation of beauty and charm events uses the fact that b quarks are much heavier than c quarks. In contrast to charmed hadrons the decay products of beauty hadrons are expected to show relatively large transverse momenta $p_\perp^{rel}$ with respect to the direction flight of the decaying particle. Since this analysis does not attempt to reconstruct beauty hadrons this direction is approximated by the thrust axis of the jet containing the muon given by

$$T = \max \frac{\Sigma \left| p_i^L \right|}{\Sigma \left| p_i \right|}, \qquad (6)$$

where the sum runs over all particles i except the muon. Here p_i and p_i^L are the momenta of the particles and their longitudinal components with respect to the thrust axis.

The optimal distinction of charm and beauty events is expected if the $p_\perp^{rel}$ of the identified charged lepton, i.e. the muon in this analysis, is considered. The $p_\perp^{\mu\ rel}$ distributions for charm and beauty events as obtained from the AROMA Monte Carlo event generator are compared in figure 6. As expected from the discussion above the $p_\perp^{\mu\ rel}$ distribution in b events is significantly harder than in c events. These shapes will be used for the extraction of the beauty production cross section.

Apart from semileptonic charm and beauty decays other hadrons do contribute to the muon sample because of misidentification. To determine this background, the probability $\mathcal{P}_h^\mu(\vec{p})$ for a

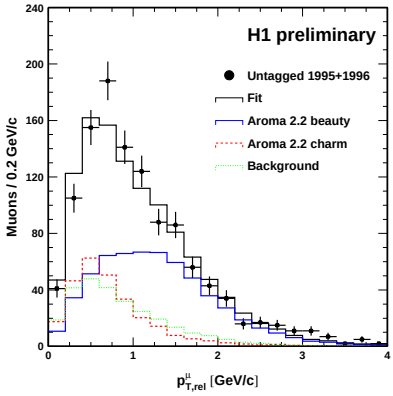

Figure 7. $p_{\perp}^{\mu\ rel}$ Distributions for charm and beauty events.

hadron $h = \pi, K, p$ being interpreted as muon has to be known precisely. These probability functions have been parameterized using Monte Carlo simulations. They are verified by studying K_s^0 and ϕ decays in data, which present unambiguous sources of pions and kaons, respectively. The probability functions vary with the polar angle, but do not exceed $6 \cdot 10^{-3}$, $2 \cdot 10^{-2}$, $2 \cdot 10^{-3}$ for pions, kaons and protons, respectively. With the knowledge $\mathcal{P}_h^{\mu}(\vec{p})$ it becomes possible to calculate the background due to faked muons in shape and absolute magnitude from the data.

The observed $p_{\perp}^{\mu\ rel}$ distribution is shown in figure 7 together with the fitted contributions of beauty and charm, using the shapes from AROMA Monte Carlo simulations, and the hadronic background determined from the data. The fitted contribution of beauty amounts to $f_b = (51.4 \pm 4.4)\%$.

The visible beauty electroproduction cross section is determined from the number of muons N_b^{μ} attributed to beauty quark decay as:

$$\sigma_{vis}(ep \to b\bar{b}X) = (0.93 \pm 0.08\ ^{+0.21}_{-0.12})\ \text{nb} \qquad (7)$$

in the visible kinematic range $Q^2 < 1$ GeV^2, $0.1 < y < 0.8$, $p_{\perp}^{\mu} > 2$ GeV and $35^o < \theta^{\mu} < 130^o$, where the first error is statistical and the second is the experimental systematic uncertainty. For the same cuts the LO AROMA Monte Carlo simulation predicts a visible cross section 0f 0.19 nb, which is about only 20% of the measured value. A NLO cross section prediction is not available yet because this requires the implementation of the weak decay in the massive calculation programs.

4. CONCLUSION

Inclusive $D^{*\pm}$ differential cross sections in DIS and photoproduction have been presented. They agree reasonably well with the massive NLO calculations. The data have been used for a direct extraction of the gluon density in the proton in both kinematic regimes. The gluon density obtained from electroproduction and photoproduction of charm agree well with each other and with that derived from the QCD analysis of the inclusive F_2. First results on the beauty photoproduction cross section have been presented using semi-muonic decays of beauty hadrons. The observed cross section is about a factor of five larger than predicted by LO QCD.

REFERENCES

1. C. Adloff *et al.* (H1), *Nucl. Phys.* **B545**(1999)21.
2. C. Adloff *et al.* (H1), ICHEP98, abstract 575.
3. I. Abt *et al.* (H1), *Nucl. Instr. Meth* **A386**(1997)348.
4. B.A. Kniehl *et al.*, *Z. Phys.* **C76**(1997)689; M Cacciari and M. Greco, *Phys. Rev.* **D55**(1997)7134; J. Binnewies *et al.*, *Z. Phys.* **C76**(1997)677.
5. J. Binnewies *et al.*, *Phys. Rev.* **D58**(1998)014014.
6. B.W. Harris and J. Smith, *Phys. Lett.* **B353**(1995)535; *Phys. Rev.* **D57**(1998)2806.
7. Leanen *et al.*, *Nucl. Phys.* **B392**(1993)162 and 229.
8. M.A.G. Aivazis *et al.*, *Phys. Rev.* **D50**(1994)3102.
9. S. Kretzer and I. Schienbein, *Phys. Rev.* **D59**(1999)54004.
10. S. Frixione *et al.*, *Phys. Lett.* **B348**(1995)633; *Nucl. Phys.* **B454**(1995)3.
11. C. Adloff *et al.* (H1), *Z. Phys.* **C72**(1996)593.
12. S. Riemersma , J. Smith, W.L. Van Neerven, *Phys. Lett.* **B347**(1995)143.